Journal of Glaciology, Vol. 39, No. 132, 1993

Instruments and Methods

Subglacial measurement of turbidity and electrical conductivity

DAN B. STONE, GARRY K. C. CLARKE AND ERIK W. BLAKE
Department of Geophysics and Astronomy, University of British Columbia, Vancouver, British Columbia V6T 1Z4, Canada

ABSTRACT. Direct measurements of the properties of subglacial water are necessary for understanding water flow beneath glaciers. In this paper we describe the construction, calibration and field usage of two instruments—one that measures turbidity and the other that measures electrical conductivity of subglacial water. The sensors are inexpensive and reliable. To demonstrate the potential usefulness of these devices, we present samples of data obtained from beneath Trapridge Glacier, Yukon Territory, Canada.

INTRODUCTION

How does water flow beneath a glacier? This question has been a focus of glaciological research for more than three decades. As a result of these efforts, various drainage-system configurations have been proposed. In many cases, field observations are explained readily by the proposed configurations. In other cases, existing theories of basal-water flow are clearly inappropriate or incomplete. This paper is intended to advance general understanding of water flow beneath glaciers by describing instruments that measure, in situ, the turbidity and electrical conductivity of subglacial water. Direct measurement of these properties at the glacier bed can lead to a more complete understanding of subglacial water flow.

Until recently, drainage-system morphologies have been inferred largely from proglacial observations. These observations tend to include measurement in outlet streams of one or more of the following quantities: tracer concentration, turbidity or electrical conductivity. The most common method for studying subglacial water flow involves determining the velocity of a tracer that has moved through the drainage system (e.g. Stenborg, 1969; Behrens and others, 1975; Burkimsher, 1983; Brugman, 1986; Seaberg and others, 1988; Willis and others, 1990). Typically, salt or a fluorescent dye is used as the tracer. Parcels of "naturally labeled" water with known, specific origins have also been used. For example, Humphrey and others (1986) used turbidity pulses in water flowing from beneath Variegated Glacier, Alaska, to estimate mean water velocity in the hydraulic system. Electrical conductivity has been used successfully by Collins (1979) as a basis for distinguishing between the surface melt and basal components of discharge from two alpine glaciers in Switzerland. An entirely different approach is to interpret former subglacial flow conditions from the occurrence and spatial distribution of surficial deposits and landforms in recently deglaciated areas (e.g. Walder and Hallet, 1979).

In an effort to apply standard proglacial techniques directly at the glacier bed, we have developed durable, inexpensive sensors that allow continuous measurement of the turbidity and electrical conductivity of subglacial water. Measurements obtained with these sensors provide direct indications of basal-water flow velocity and subglacial provenance. In the following sections, we describe the construction, calibration and field usage of these sensors. Data collected at the bed of Trapridge Glacier, Yukon Territory, demonstrate the usefulness of these devices.

TURBIDITY

Description of the device

The basic components of the turbidity sensor are a light source, two photodetectors and a voltage regulator (Fig. 1a). For the light source, we use a miniature incandescent lamp manufactured by Spectro (part No. 8097). This source provides nearly spherical illumination, thereby reducing geometric constraints on construction. Because the intensity of an incandescent source will change if the supply voltage varies or if the filament degrades, we use two detectors—a reference detector that monitors an internal light path through the sensor and a sample detector that monitors a light path through the water gap. We use photo-Darlington detectors (Motorola, part No. MRD711) having a spectral response centered at ~940 nm. These detectors are amplified phototransistors and act as current sources, passing a current proportional to the flux of infrared-wavelength photons incident upon the transistor base.

In constructing turbidity sensors, caution must be exercised to prevent the detectors from operating under optically saturated conditions; this is especially important for the reference detector. Under saturated conditions, detectors are insensitive to changes of source intensity. To prevent saturation, we have found that the intensity of incident light can be reduced, when necessary, by

https://doi.org/10.3189/S0022143000016075 Published online by Cambridge University Press

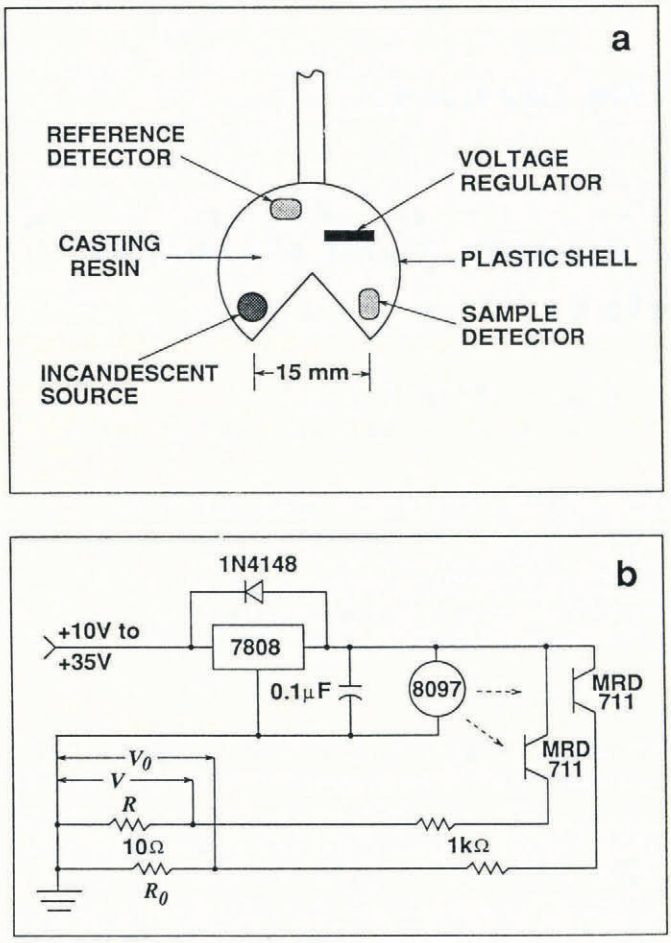

Fig. 1. Turbidity sensor schematic and circuit diagram showing the relative positions and physical connections of electronic components. a. The basic components are an incandescent light source, two infrared photo-Darlington detectors — one for the reference light path and one for the light path through the water sample — and a voltage regulator. These components are housed in a plastic shell and then sealed in a casting resin that does not degrade in the presence of mineralized water. b. Circuit diagram for turbidity sensor and voltage measurement. Shown in this diagram are the unregulated supply voltage from the surface (upper left), the sensor components (middle and right) and the surface-voltage measurement circuit (lower left).

partially covering the detector faces with small pieces of black electrical tape.

If the sensor is in thermal equilibrium with its surroundings, variations in reference measurements result only from changes in source intensity, assuming that there is no variation in ambient light. Sample detector measurements depend on the source intensity and on the number of infrared-wavelength photons that pass through the water gap; more photons reach the sample detector when the path is unobstructed than when intervening scatterers are present. As explained below, turbidity measurement is based on the ratio of currents from the reference and sample detectors.

A series 7800 voltage regulator provides a constant 8 V supply for the light source and for collector inputs of the detectors (Fig. 1b). By including the regulator as part of the sensor assembly, voltage variations due to different lead-wire lengths or changes in voltage of the surface power supply are unimportant, provided that the regulator is adequately supplied. In addition to the basic components, a small signal diode (1N4148) and a capacitor (0.1 μF) are used to protect and stabilize the regulator (Horowitz and Hill, 1989, p. 341). Two 1 kΩ resistors serve as loads on the emitter outputs of the detectors. To minimize wire costs, the entire circuit operates on four conductors: one for each detector, one for the voltage regulator supply and one for ground.

As shown in Figure 1a, the sensor components are housed in a spherical shell from which a wedge has been cut; table-tennis balls work well for this purpose. Our design has two important features: it is small enough to fit down unreamed boreholes and the wedge-shaped water gap reduces the possibility that the sample path will become clogged. The electronic components inside the plastic shell are sealed in a casting resin. In selecting a casting material, chemical reactions of the resin with mineralized water must be considered. We have found that Sun Cure — a clear laminating resin available from Industrial Formulators of Canada — is excellent. The sensor is cast in a two-stage process. First, the sensor is positioned so that one of the planes forming the wedge provides a level surface; one half of the sensor is then filled with resin and allowed to harden. When this stage is finished, the sensor is rotated so that the other wedge plane is horizontal, and the remaining part of the sensor is cast.

Calibration

Turbidity is usually defined as the reduction in intensity of a beam of light passing through a suspension:

$$\frac{\mathcal{I}}{\mathcal{I}_0} = \exp(-\tau L) \qquad (1)$$

where $\mathcal{I}$ is the intensity of light after passing through a length L of suspension, $\mathcal{I}_0$ is the intensity of the unobstructed light beam and τ is the turbidity (Kerker, 1969; Melik and Fogler, 1983; Gregory, 1985). In general, phototransistors have non-linear behavior over the full collector–emitter voltage range. However, for small changes, the response is approximately linear (Bliss, 1983 p. 4–13). Under these conditions, there is a direct relation between the photo-induced current I and the intensity of incident light, $I \propto \mathcal{I}$, and Equation (1) can be rewritten as

$$\frac{I}{I_0} = \exp(-\tau L) \qquad (2)$$

where I_0 is the current induced by the unobstructed light beam. To use this expression, the value of I_0 must be known. However, we cannot measure simultaneously the intensity of incident light through both "clear" and turbid paths with the same detector. Thus, we employ the reference detector to monitor an internal path and provide an approximate measure of I_0. Solving Equation (2) for τ, and using Ohm's law to rewrite current in terms of voltage V and resistance R, we obtain

$$\tau = -\frac{1}{L}\ln\left(\frac{R_0 V}{R V_0}\right). \qquad (3)$$

In Equation (3), subscripted quantities refer to the

https://doi.org/10.3189/S0022143000016075 Published online by Cambridge University Press

reference circuit. The turbidity sensors we have described employ nearly identical components in close proximity. Under these conditions $R_0 \approx R$, and the last expression reduces to

$$\tau = -\frac{1}{L}\ln\left(\frac{V}{V_0}\right). \quad (4)$$

There are several factors that complicate measurement of the actual intensity of the undisturbed beam by the reference detector: (1) the source may not be a perfect isotropic radiator; (2) the detectors are not identical and may not be optimally oriented; (3) the separation distances between the source and each detector may be different; and (4) the reference and sample light paths can have different optical properties, even when the sensor is not in a suspension. For these reasons, we include a positive constant a that multiplies the reference voltage—in essence allowing correction of the measured reference intensity. With this modification, Equation (4) becomes

$$\tau = -\frac{1}{L}\ln\left(\frac{V}{aV_0}\right). \quad (5)$$

It is possible to estimate the value of a for a given sensor by measuring the voltages from both detectors when the sensor is in "clear" water. In this case $\tau \approx 0$ and, from Equation (5), we see that $a = V/V_0$. We have made these measurements for a number of sensors and have found that values of a are in the range $0.6445 \leq a \leq 1.006$. For some of our early, prototype sensors, the necessary calibration measurements were not made; when this information is unavailable, we ordinarily set $a = 1$. Equation (5) defines our usage of the term "turbidity". With this relation, turbidity-sensor calibration entails measuring the water-gap path length L and estimating a reference intensity correction value for the constant a.

For subglacial measurements, a calibration relating τ to suspended-sediment concentration is unrealizable, because it requires detailed knowledge of suspension properties or representation of the suspension based on a limited number of samples. We have made numerous laboratory tests in which the suspended-sediment concentration, for a given grain-size distribution, was controlled carefully. Our investigations have shown that turbidity depends strongly on the grain-size distribution of the suspension; smaller grains comprising less total mass can produce turbidity values much greater than larger grains having more total mass. To be fully accurate, the size, number concentration and light-scattering properties of all particles in the suspension must be known at all times. This requirement is further complicated if the suspension is not uniformly mixed. Because such information is unavailable, turbidity sensors are sometimes calibrated by collecting samples of the suspension while readings are being made, then analyzing the samples to determine sediment concentration (e.g. Humphrey and others, 1986). Whereas this procedure may be suitable for surface streams, it cannot be applied to subglacial water flow because a large number of samples cannot be easily collected from the glacier bed and samples that are collected will likely be altered by the time they reach the glacier surface. Thus, we have not used turbidity readings to estimate the suspended-sediment concentration of subglacial water.

ELECTRICAL CONDUCTIVITY

Description of the device

The electrical-conductivity sensor consists of two parallel, cylindrical electrodes embedded side-by-side in a non-conducting material and housed in a protective tube (Fig. 2). The electrodes are stainless steel rods 6.35 mm (0.25 in) in diameter and 76.2 mm (3.0 in) long. They are press-fitted into a pre-drilled, solid nylon cylinder having a diameter of 25.4 mm (1.0 in) and a length of 50.8 mm (2.0 in). The rods extend 6.35 mm (0.25 in) from the measurement end of the nylon cylinder and are separated by a center-to-center spacing of 12.7 mm (0.5 in). To allow solder connections for lead wires, small brass pins are inserted into the interior ends of the rods. The brass pins are placed in pre-drilled holes and fixed to the rods with a flux and low-temperature solder that bonds to stainless steel. The entire assembly is placed in a section of ABS or PVC conduit 101.6 mm (4.0 in) long and having an inside diameter of 25.4 mm (1.0 in). The conduit is then filled with an electrically insulating casting resin. Important features of this design are similar to those previously discussed for our turbidity sensors: small size and a geometry that reduces the possibility of clogging. Additionally, the use of stainless steel minimizes electrode corrosion.

Calibration

A standard reference solution is required for conductivity-sensor calibrations. We prepare our own reference solutions using potassium chloride and freshly distilled water but conductivity standards are also available from commercial suppliers. According to Jones and Bradshaw

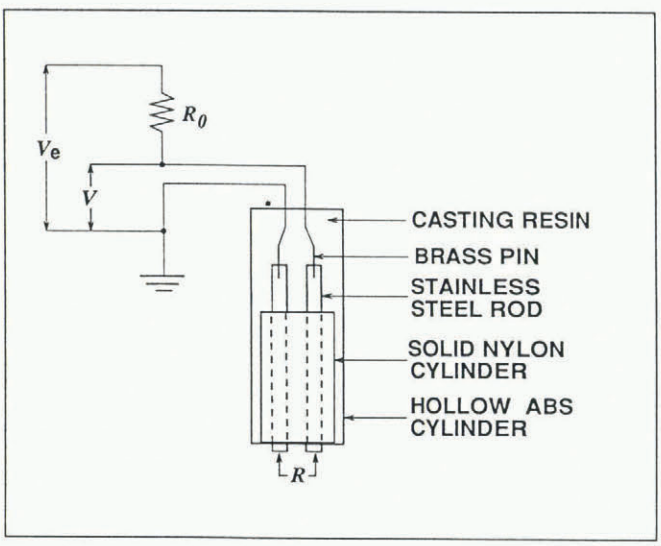

Fig. 2. Electrical-conductivity sensor showing the basic design and measurement circuit. Stainless steel rods are press-fitted into a pre-drilled, solid nylon cylinder. To allow solder connections for lead wires, brass pins are inserted into the interior ends of the rods. The entire assembly is placed in a section of ABS or PVC conduit, which is then filled with casting resin. With this device, the conductance of basal water can be determined by means of an a.c. half-bridge measurement.

https://doi.org/10.3189/S0022143000016075 Published online by Cambridge University Press

(1933), a 1 kg solution containing 0.745263 g of KCl in distilled water in a vacuum will have a conductivity of $0.07736\,S\,m^{-1}$ at 0°C. Our standard solutions are prepared in air by dissolving ~0.7452 g of KCl in enough distilled water to yield exactly 1 litre. The conductivity of our standard solution differs slightly from that described by Jones and Bradshaw (1933) because we have implicitly assumed that 1 litre of solution weighs exactly 1 kg and we have not applied a vacuum correction. Nevertheless, discrepancies arising from differences in the preparation procedures are small and do not influence calibration accuracy appreciably.

The reference solution is used to obtain a cell-constant value for each sensor. The cell constant K_c is the constant of proportionality between conductivity σ and conductance G:

$$\sigma = K_c G. \tag{6}$$

The cell constant depends on sensor geometry and has dimensions (L^{-1}). For simple geometries, K_c can be determined analytically, if the inter-electrode distance and electrode surface areas are known. Unfortunately, conductivity sensors having simple geometries, such as parallel plates or concentric cylinders, tend to accumulate debris between the electrodes when used in a glacial environment. Our sensors have been designed to avoid clogging. Because of this design, the cell constants cannot be determined analytically. Thus, values for K_c are found by submerging the electrodes in the standard solution and measuring the resistance R between them. Since $G = 1/R$, these resistances are multiplied by the known conductivity σ_s of the standard solution to obtain the cell constants:

$$K_c = R\sigma_s. \tag{7}$$

Electrical conductivity of aqueous solutions is strongly dependent on temperature because the conduction process is electrolytic and ion mobility always increases with temperature. To minimize the effects of temperature variation, our standard solution is held constant at 0°C throughout the calibration procedure. To achieve this, we pass a cooled fluid through a curved copper tube that has been placed in the bottom of the solution container. The solution is continuously stirred during calibrations to ensure a uniform temperature distribution.

In a given year, all sensors are calibrated simultaneously in the same solution. Typically, we record solution temperature and sensor readings at 2 min intervals for at least 40 min using Campbell CR10 dataloggers. To approximate the conditions under which our sensors are used in the field, we apply an excitation of 250 mV and use a nominal reference resistance of 10 kΩ (±2%) for each sensor. (The measurement procedure is described in the following section.) For each sensor, the mean value of the set of measurements is computed. These values are then used to calculate individual cell constants according to Equation (7).

FIELD USAGE

Installation

We position our sensors ~0.25–0.5 m above the bottom of the borehole. If a sensor is placed too low, it may become packed with debris or sheared by glacier motion; if a sensor is placed too high, it will be removed from the active-flow region. For solitary sensors, weight must be added to promote sinking. If both turbidity and electrical-conductivity sensors are to be installed in the same borehole, we usually place the conductivity sensor immediately above the turbidity sensor and fix their relative positions using self-vulcanizing tape. Once in place, the sensors are tethered by their lead wires to an ice screw at the surface.

Measurement procedures

As illustrated in Figure 1b, a turbidity reading is obtained by measuring the voltage drop across a 10 Ω precision resistor for both the reference and sample detectors. The measured voltages are used with Equation (5) to calculate turbidity. Before the first measurement is made, the lamp is turned on and allowed to warm up for 2 s. We delay 0.5 s between measurements to allow switching transients to decay. Power to the sensor is then turned off until the next measurement is to be made.

Electrical conductivity is measured using the circuit shown in Figure 2. To avoid polarization effects, the sensor voltage is measured twice in quick succession, with the excitation-voltage polarity reversed between measurements. The two readings are averaged to obtain a single value. This procedure constitutes an a.c. half-bridge measurement and is a standard function on Campbell dataloggers (Campbell Scientific, 1989). The conductance is obtained from the following relation:

$$G = \frac{1}{R_0}\left(\frac{V_e}{V} - 1\right) \tag{8}$$

where V_e is the excitation voltage, V is the measured voltage and R_0 is the reference resistance. Conductance values, obtained by this procedure, are combined with the known cell constants according to Equation (6) to obtain conductivity. For optimal performance, values of V_e and R_0 should be chosen to maximize output fluctuations within the measurement range. Typically, we use an excitation voltage of $V_e = 250$ mV and a reference resistance of $R_0 = 10$ kΩ.

RESULTS AND DISCUSSION

Examples of data collected using the sensors described in this paper are shown in Figures 3 and 4. These data were collected from beneath Trapridge Glacier, Yukon Territory. They are presented here to illustrate the types of responses that we have recorded with our sensors; thus, only brief interpretations are given. The interval between individual measurements for the data shown in these figures is 2 min. For ease of plotting, we have omitted every second data point from these records.

A range of subglacial turbidity signals is shown in Figure 3. The small-amplitude diurnal fluctuations shown in Figure 3a are known to be associated with hydraulic-head gradient, which we have computed from basal-water pressure measurements; turbidity is maximum when the gradient is largest and is minimum when the gradient is smallest. Such correspondence indicates that

https://doi.org/10.3189/S0022143000016075 Published online by Cambridge University Press

turbidity signals of this type are associated with water flow. The general rising trend apparent in this signal is due to chemical interaction of the 1989 casting resin with basal water—confirmed by removal and post-mortem examination of another 1989 sensor. This deficiency was corrected in subsequent years.

A large-amplitude turbidity event is illustrated in Figure 3b. Prior to this event, there were no indications of subglacial water flow; evidence from this, and other sensors, suggests that basal water was ponded over a part of the glacier bed. The rapid rise in turbidity coincided with large changes in basal-water pressure and electrical conductivity, as observed by many sensors in different locations. Following this event, a release of basal water was recorded in a proglacial outlet stream and subglacial sensors indicated a return to ponded conditions. These observations suggest that a sudden and temporary rearrangement of the drainage system took place and was accompanied by release of stored basal water.

A large turbidity rise, followed by a period of small-amplitude diurnal oscillations, is evident in Figure 3c. In this case, a change in subglacial flow conditions—less abrupt and longer lasting than that shown in Figure 3b—is indicated. Signals of this type could be produced if water-flow passageways developed in the vicinity of the sensor or if the sensor was carried by glacier motion over an area in which drainage was already established.

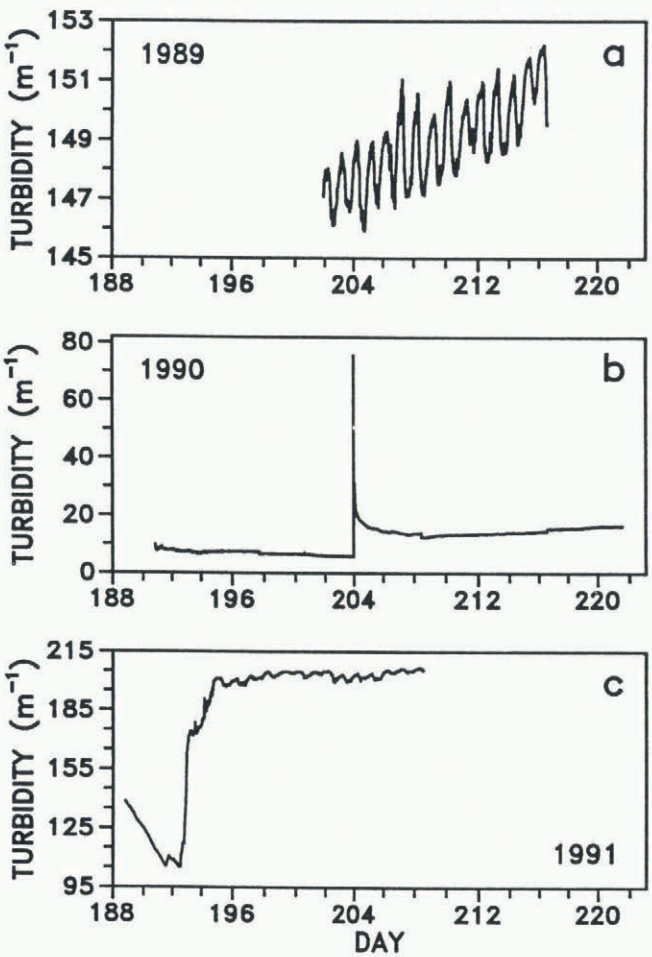

Fig. 3. Observations of subglacial turbidity from different sensors beneath Trapridge Glacier, Yukon Territory, during three consecutive field seasons: 1989 (a), 1990 (b) and 1991 (c). Day 188 corresponds to 7 July. These data illustrate the wide range of responses that we have measured with our sensors—from small-amplitude diurnal fluctuation (a), to large-amplitude turbidity events (b). Both response types are evident in (c).

Typical subglacial conductivity records for Trapridge Glacier are shown in Figure 4. The S.I. unit for electrical conductivity is Siemens per meter ($S\,m^{-1}$); we have expressed our results as micro-Siemens per centimeter ($\mu S\,cm^{-1}$) because this is the more commonly used unit. The data shown in Figure 4a were obtained from a sensor that had been in place at the glacier bed for a full year; this sensor was originally installed and used in 1989. At the beginning of the 1990 field season, the lead wires to this sensor were uncovered at the glacier surface and the sensor was re-attached to a data logger. The large drop in conductivity on day 204 coincides with the turbidity event that was discussed in connection with Figure 3b. Reduction in electrical conductivity suggests that an infusion of fresh surface water—thereby diluting mineralized basal water—accompanied this event.

A long period of gradually increasing conductivity is shown in Figure 4b. Similar trends, on various timescales, are also evident in Figure 4a. Such behavior may indicate increasing ion concentration with increasing contact time between water and basal sediments; in hydrology, it is well known that the conductivity of storm run-off or ground water depends on the amount of time spent in contact with sediments (e.g. Pilgrim and others, 1979). Note that the increase in conductivity on day 192 coincides with rising turbidity, as shown in Figure 3c. Unlike the 1990 "event" illustrated in Figures 3b and 4a in which there was an inverse relation between turbidity and conductivity, the data in 1991 show a direct correspondence. In contrast to the 1990 example, the direct relationship suggests that the two 1991 sensors were hydraulically isolated from each other but were still subjected to the same glacier forcings.

We have run sensors of both types at intervals ranging from 2 to 20 min for more than a year without failure. The continuous records shown in Figures 3 and 4 are evidence of the reliability and longevity of our sensors. Another attractive feature of these sensors is their low cost; the parts for either sensor can be obtained for roughly U.S. $10.

Because of their low cost, it is feasible to deploy subglacial arrays of turbidity and electrical conductivity sensors. Arrays of these sensors can be used to estimate the rate and direction of water flow at the bed. For instance, when boreholes connect with the subglacial drainage system, nearby sensors register turbidity and conductivity pulses. We have employed conductivity sensors in borehole-to-borehole tracer tests successfully, using ordinary table salt as the tracer. The data shown in Figure 4 suggest that electrical conductivity may also be used to estimate the residence time of subglacial water.

CONCLUDING REMARKS

In some respects the subglacial environment is better suited than the subaerial one for measurements of turbidity and electrical conductivity. Although risk of

https://doi.org/10.3189/S0022143000016075 Published online by Cambridge University Press

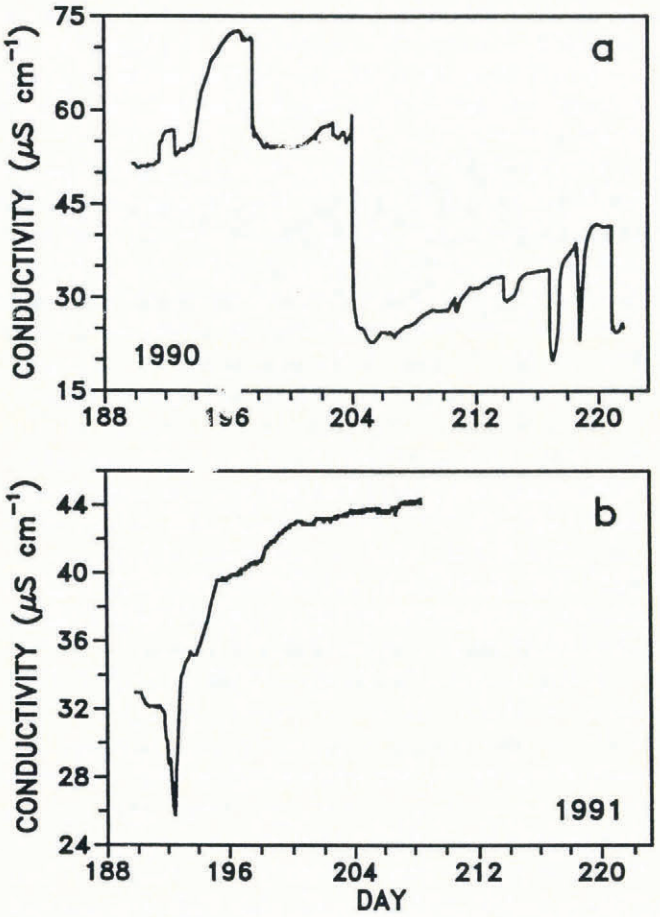

Fig. 4. Electrical conductivity of water beneath Trapridge Glacier measured with different sensors in 1990 (a) and 1991 (b). Day 188 corresponds to 7 July. The data shown in (a) were obtained from a sensor that was installed during the 1989 field season. Note that in (a) the large conductivity decrease on day 204 coincides with the turbidity pulse shown in Figure 3b.

mechanical destruction is a concern, the absence of thermal fluctuations is advantageous to both turbidity and conductivity sensors. For turbidity sensors, the complete absence of ambient light is a major benefit. Lastly, and of greatest importance, the best approach to studying subglacial drainage is to monitor water flow in situ, rather than rely on inferences based on proglacial observations.

ACKNOWLEDGEMENTS

Support for this research has been provided by the Natural Sciences and Engineering Research Council of Canada, the University of British Columbia and Geddes Resources Limited. The data presented in this paper were collected in Kluane National Park. We thank Parks Canada and the Yukon Territorial Government for granting permission to conduct field studies in the park. We are indebted to F. Jones for laying the ground work upon which our turbidity sensor was founded, and to D. Schreiber and W. Siep for the meticulous care that they have taken in constructing each and every conductivity sensor.

REFERENCES

Behrens, H., H. Bergmann, H. Moser, W. Ambach and O. Jochum. 1975. On the water channels of the internal drainage system of the Hintereisferner, Ötztal Alps, Austria. *J. Glaciol.*, **14**(72), 375–382.

Bliss, J. 1983. *Motorola optoelectronics device data.* Phoenix, AZ, Motorola.

Brugman, M. M. 1986. Water flow at the base of a surging glacier. (Ph.D. thesis, California Institute of Technology.)

Burkimsher, M. 1983. Investigations of glacier hydrological systems using dye tracer techniques: observations at Pasterzengletscher, Austria. *J. Glaciol.*, **29**(103), 403–416.

Campbell Scientific. 1989. *CR10 measurement and control module operator's manual.* Logan, UT, Campbell Scientific.

Collins, D. N. 1979. Quantitative determination of the subglacial hydrology of two Alpine glaciers. *J. Glaciol.*, **23**(89), 347–362.

Gregory, J. 1985. Turbidity fluctuations in flowing suspensions. *J. Colloid Interface Sci.*, **105**(2), 357–371.

Horowitz, P. and W. Hill. 1989. *The art of electronics.* Cambridge, Cambridge University Press.

Humphrey, N., C. Raymond and W. Harrison. 1986. Discharges of turbid water during mini-surges of Variegated Glacier, Alaska, U.S.A. *J. Glaciol.*, **32**(111), 195–207.

Jones, G. and B. C. Bradshaw. 1933. The measurement of the conductance of electrolytes. V. A redetermination of the conductance of standard potassium chloride solutions in absolute units. *J. Am. Chem. Soc.*, **55**, 1780–1800.

Kerker, M. 1969. *The scattering of light and other electromagnetic radiation.* New York, Academic Press.

Melik, D. H. and H. S. Fogler. 1983. Turbidimetric determination of particle size distributions of colloidal systems. *J. Colloid Interface Sci.*, **92**(1), 161–180.

Pilgrim, D. H., D. D. Huff and T. D. Steele. 1979. Use of specific conductance and contact time relations for separating flow components in storm runoff. *Water Resour. Res.*, **15**(2), 329–339.

Seaberg, S. Z., J. Z. Seaberg, R. LeB. Hooke and D. W. Wiberg. 1988. Character of the englacial and subglacial drainage system in the lower part of the ablation area of Storglaciären, Sweden, as revealed by dye-trace studies. *J. Glaciol.*, **34**(117), 217–227.

Stenborg, T. 1969. Studies of the internal drainage of glaciers. *Geogr. Ann.*, **51A**(1–2), 13–41.

Walder, J. and B. Hallet. 1979. Geometry of former subglacial water channels and cavities. *J. Glaciol.*, **23**(89), 335–346.

Willis, I. C., M. J. Sharp and K. S. Richards. 1990. Configuration of the drainage system of Midtdalsbreen, Norway, as indicated by dye-tracing experiments. *J. Glaciol.*, **36**(122), 89–101.

The accuracy of references in the text and in this list is the responsibility of the authors, to whom queries should be addressed.

MS received 10 March 1992 and in revised form 12 May 1992

https://doi.org/10.3189/S0022143000016075 Published online by Cambridge University Press